Ultrafast laser-induced coherent spin dynamics in ferromagnetic $Ga_{1-x}Mn_xAs$/GaAs structures

J. Qi,[1] Y. Xu,[1] A. Steigerwald,[1] X. Liu,[2] J. K. Furdyna,[2] I. E. Perakis,[3] and N. H. Tolk[1]
[1]*Department of Physics and Astronomy, Vanderbilt University, Nashville, Tennessee 37235, USA*
[2]*Department of Physics, University of Notre Dame, Notre Dame, Indiana 46556, USA*
[3]*Department of Physics, Foundation for Research and Technology-Hellas, Institute of Electronic Structure and Laser, University of Crete, Heraklion, 71110 Crete, Greece*
(Received 14 October 2008; revised manuscript received 5 December 2008; published 3 February 2009)

Ultrafast pump-probe magneto-optical spectroscopy is used to study coherent spin dynamics in ferromagnetic semiconductor $Ga_{1-x}Mn_xAs$ systems at excitation photon energies E_{ph} both above and below the band gap E_g of GaAs. Above E_g, the temporal Kerr rotation signal is found to be strongly dependent on pump photon polarization. This polarization dependence, persisting to room temperature, is attributed to spins of electrons photoexcited to the conduction band, and disappears for $E_{ph}<E_g$. Below the Curie temperature T_C of the $Ga_{1-x}Mn_xAs$ samples, the temporal Kerr rotation acquires an additional oscillatory component with a period of the order of 100 ps, attributed to the precession of the ferromagnetically coupled Mn spins. This precession is observed for excitation both above and below E_g, regardless of the pump polarization states. The detailed characteristics of this ferromagnetic precession are discussed in terms of the Landau-Lifshitz-Gilbert model. In discussing the observed results, special attention is given to the process of the magnetization precession due to excitation of the pump, to its dependence on the pump intensity, and ambient temperature, and to the relationship between the damping of the magnetization precession and the defects characteristic of ferromagnetic GaMnAs.

DOI: 10.1103/PhysRevB.79.085304 PACS number(s): 78.47.J−, 75.50.Pp, 75.30.Gw, 78.20.Ls

I. INTRODUCTION

In recent years, ultrafast nonequilibrium and dynamic properties of a wide variety of magnetically ordered systems have been investigated, and as a consequence, useful insights into future applications in novel magnetic devices have been obtained.[1–4] At the same time, ferromagnetic (FM) semiconductor materials such as GaMnAs have attracted intense interest because of their potential for spintronics applications based on the interaction between charge-carrier spins and localized FM-ordered magnetic moments.[5,6] Recently, by using ultrafast pump-probe magneto-optical spectroscopy, several research groups have reported a variety of different collective magnetic phenomena in GaMnAs.[3,7–16] The magnetization dynamics identified by these methods suggest the existence of two temporal regimes in the photoexcited GaMnAs system: a "fast regime" (femtosecond or subpicosecond) and a "slow regime" (picosecond to nanosecond). In the subpicosecond regime, depending on the photoexcitation intensity, much research has focused on light-induced demagnetization and on thermal/nonthermal effects in magnetization dynamics.[3,17–19] The slow (picosecond to nanosecond) regime, on the other hand, is dominated by coherent dynamics of carriers and Mn spins,[7–16] where the precession of the ferromagnetically coupled Mn spins (i.e., of the sample magnetization) due to light-induced transient reorientation of the magnetic easy axis has been observed. However, the interpretation of the experimental observations in both temporal regimes is still a matter of debate.

In this paper we present a study of photoinduced dynamics of both carrier spins and local Mn spins using time-resolved magneto-optical Kerr effect (TR-MOKE) spectroscopy. Specifically, we present a comprehensive study of the magnetization precession in the nanosecond regime as function of ambient temperature T_0, pump intensity I, and photon energy E_{ph}. As detailed in the discussion sections, the observed results involving magnetization dynamics and its relaxation can be understood in terms of the Landau-Lifshitz-Gilbert picture.

II. EXPERIMENTAL CONFIGURATION

The $Ga_{1-x}Mn_xAs$ samples used in this study were grown by low-temperature molecular-beam epitaxy (LT-MBE), which is employed in order to circumvent the problems of low solubility and precipitation of Mn at normal growth conditions. Before the growth of the $Ga_{1-x}Mn_xAs$ layer, two buffer layers—a normal GaAs (~600 °C) and a low-temperature GaAs (~270 °C)—were consecutively grown on a semi-insulating GaAs(001) substrate. The growths of $Ga_{1-x}Mn_xAs$ are carried out under same condition for all samples. The surface quality of the samples is monitored *in situ* by reflection high energy electron diffraction (RHEED). During the LT-MBE the RHEED pattern typically shows a (1×1) surface reconstruction for LT-GaAs, and a (1×2) reconstruction for (Ga,Mn)As. During the growth of $Ga_{1-x}Mn_xAs$ one can monitor the oscillations of the intensity of the specular RHEED spot (so-called "RHEED oscillations") are seen, which indicate that the growth proceeds layer by layer, with two-dimensional nucleation. The crystallographic structure of the samples has been investigated by x-ray diffraction (XRD). No second phase is observed in XRD study. In addition, Pendellösung fringes are clearly observed in all samples, indicating a very high quality single crystalline epitaxial layer with smooth interfaces and uniform composition. The results of XRD are also used for determining the lattice constants and the Mn concentrations of $Ga_{1-x}Mn_xAs$ layers. Partial sections of samples are annealed

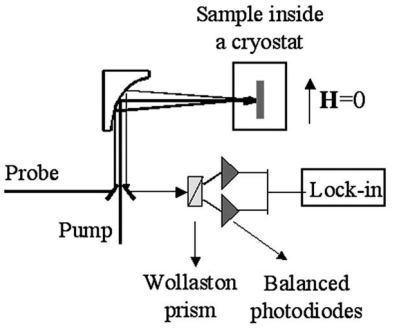

FIG. 1. Schematic representation of the experimental configuration for time-resolved Kerr rotation measurements.

for 1 h around 280 °C at the same fixed flow of N_2 gas of 1.5 standard cubic feet per hour (SCFH), for improving both the Curie temperature and the crystallinity of $Ga_{1-x}Mn_xAs$. Magnetoresistance, Hall measurements, and superconducting quantum interference device (SQUID) magnetometry are performed for all samples for electrical and magnetic characterization of $Ga_{1-x}Mn_xAs$ layers, including the determination of their Curie temperature T_C. Note that the magnetization measurements show similar results as that described in considerable detail in earlier reports.[20] In this study we mainly investigate two ferromagnetic samples: sample A: $Ga_{0.964}Mn_{0.036}As$ annealed at 286 °C, with a Curie temperature $T_C \approx 80$ K, and a thickness of 98 nm; and sample B: as-grown $Ga_{0.965}Mn_{0.035}As$ with $T_C \approx 52$ K and a thickness of 300 nm. Similar results were also observed on other ferromagnetic $Ga_{1-x}Mn_xAs$ samples with different Mn concentrations x, as described below.

All TR-MOKE measurements were performed using a Ti:Sapphire laser system producing ~150 fs-wide pulses with a repetition rate of 76 MHz and with a tuning range from ~720 nm (1.72 eV) to ~950 nm (1.31 eV). The pump and probe beams can either have the same photon energy, or can be tuned to different frequencies by a β-BaB_2O_4 (BBO) crystal in the pump or the probe path to double the photon energy. Here we report results obtained in one-color experiments. The pump beam, which is incident perpendicular to the sample plane, can be adjusted to be linearly, right-circularly ($\sigma+$), or left-circularly ($\sigma-$) polarized, with a typical fluence of $I_0=0.75$ $\mu J/cm^2$ (up to ~10 $\mu J/cm^2$). The probe beam used to detect magnetization dynamics by measuring the Kerr rotation angle (θ_K) or the Kerr ellipticity (ε_K) is linearly polarized and is nearly perpendicular to the film. All the experimental data were measured with no applied external magnetic field, except when noted in the text. Figure 1 shows a schematic of a typical setup used for time-resolved Kerr rotation (TRKR) measurements.

III. EXPERIMENTAL RESULTS AND ANALYSIS

A. TR-MOKE measurements at E_{ph} greater than the GaAs bandgap, E_g

We first describe one-color time-resolved magneto-optical Kerr effect measurements on samples A and B carried out at 10 K at the photon energy 1.57 eV, i.e., above the GaAs band

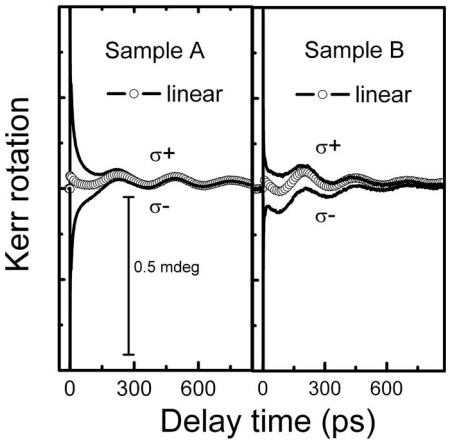

FIG. 2. Time-resolved Kerr rotation data for ferromagnetic samples A and B measured at 10 K and at photon energy 1.57 eV for different pump polarizations. Open circles are for excitation by linearly polarized laser pump pulses.

gap E_g ($E_g \approx 1.53$ eV at 10 K). The temporal Kerr rotation signals observed for left and right-circularly polarized pump light are shown in Fig. 2. The measured results show a clear decay background within ~100 ps in the time domain. The decay backgrounds from left- and right-circularly polarized light excitations are near symmetric in a given sample. In addition, at all polarizations there is a superimposed oscillatory tail with a period of the order of 100 ps. Curves obtained with linearly polarized excitation show only the oscillatory features with the same period and the same phase. In our work, the nonoscillatory decay features induced by the circularly polarized pump beam are found to persist at all temperatures studied (up to 295 K). However, it is important to note that the oscillatory behavior is observed only at temperatures below T_C.

Based on the relevant optical selection rules in the host GaAs and the very short lifetime of photoexcited coherent hole spins (of the order of ~10 femtoseconds),[21–23] we can attribute the decay backgrounds to circularly polarized light-induced coherent electron-spin dynamics in the conduction band of the Mn-doped GaAs systems. To study this in more detail, we carried out temperature-dependent measurements of coherent electron-spin decay, where the pump beam was modulated by a photoelastic modulator (PEM), which serves to remove the in-phase oscillatory behavior.[24] The experimental results for sample A (annealed) are shown in Fig. 3(a). The curve can be satisfactorily fitted by two exponentially decaying components: $\Sigma_{j=1}^{2} A_j \exp(-t/\tau_j)$.[9] The decay time τ_1 is found to be of the order of ~0.5 ps at all studied temperatures, and may be attributed to the trapping processes.[9] On the other hand, the longer relaxation time τ_2 obtained from the fitting process varies little at temperatures below and near T_C, but decreases rapidly at higher temperatures ($T > T_C$). The fact that the relaxation time τ_2 is almost constant near T_C is consistent with what was reported in Ref. 9. We carried out the same experiment on the corresponding as-grown $Ga_{0.964}Mn_{0.036}As$ sample. The results are shown in Fig. 3(b). Note that no significant difference can be seen in the damping time of the nonoscillatory component of the two

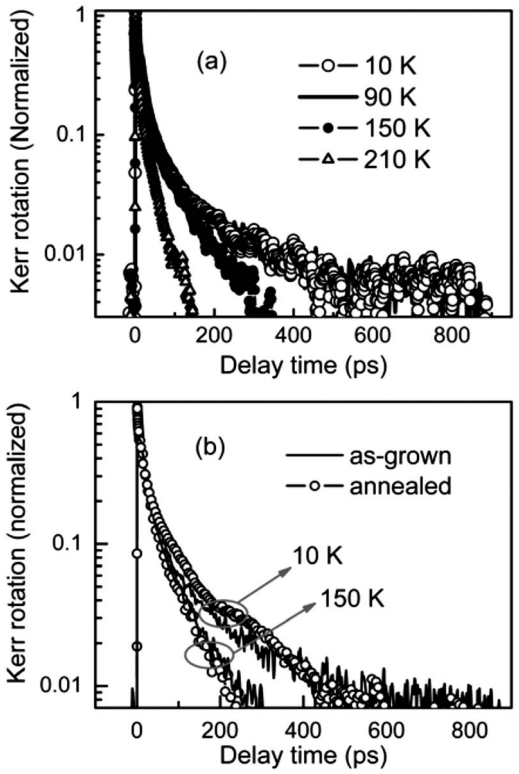

FIG. 3. (a) Temporal Kerr rotation profiles (excluding the oscillatory component) at several ambient temperatures for the annealed sample A; (b) temporal Kerr rotation profiles (excluding the oscillatory component) at two ambient temperatures for the annealed sample A (open circles) and its corresponding as-grown sample (continuous curves).

samples for a given temperature. Thus the annealing procedures (and the annealing-induced changes in magnetic properties that follow) appear to have little or no effect on the spin relaxation of the conduction electrons.

As opposed to the carrier spin phenomena, the observed oscillatory behavior can only arise from the coherent Mn spins in the presence of ferromagnetic order in the $Ga_{1-x}Mn_xAs$ samples. To understand this experimental result, it is useful to recall the different stages of time evolution of the GaMnAs system following photoexcitation. Initially, an ultrashort laser pulse creates an ensemble of nonequilibrium excited carriers with a well-defined coherent phase relationship. These coherent states may quickly become decoherent (on a femtosecond time scale) due to scattering processes between carriers involving electron-electron, hole-hole, and electron-hole scatterings. In this time regime, the energy distribution function cannot, strictly speaking, be characterized by a temperature, even though the total excess energy of the carrier system is conserved. Due to scattering among carriers, the energy of the carrier system is redistributed, leading to the creation of a hot carrier Fermi-Dirac distribution on a subpicosecond time scale.

Under these conditions, the density of phonons increases rapidly due to the carrier-phonon interaction. The carrier system transfers its excess energy to the lattice within a few picoseconds, primarily in the form of optical phonons, followed by a decay to acoustic phonons. Before equilibration is reached, the temperature characterizing the thermalized distribution function of carriers is initially higher than that of the lattice system. In this regime, the photoexcited system can be phenomenologically characterized by two effective temperatures: the carrier temperature $T_{e/h}$, and the lattice temperature T_l. Correspondingly, there are two specific heats: the carrier specific heat $C_{e/h}$, and the lattice specific heat, C_l. Somewhat later, the carrier system equilibrates with the lattice system, which leads to the same quasiequilibrium temperature for both systems. By recombination and thermal diffusion processes, the system finally returns to full thermodynamic equilibrium.

In the ferromagnetic $Ga_{1-x}Mn_xAs/GaAs$ system, it is important to note that following excitation—both in the early nonthermal time regime (as described above), and in the later quasithermal time regime—the magnetic anisotropies will differ from their initial states. As is presently understood, these differences may be due either to an enhancement of the hole concentration Δp,[25–27] or to a transient temperature elevation (ΔT),[20,25] or both. Below the Curie temperature T_C the magnetic equilibrium configuration corresponds to an in-plane orientation of the easy axis that can be specified by an angle Φ with respect to the [110] direction. This easy-axis direction depends on the interplay between the in-plane uniaxial anisotropy constant K_u and the first-order cubic anisotropy constant K_{c1}.

In static experiments performed at low temperatures, Φ, which characterizes the direction of the easy axis is found to range from approximately zero (the [110] direction) at $T_C/2$ to $\pi/4$ (the [100] direction) as the temperature decreases.[20] Φ remains close to zero for temperatures higher than $T_C/2$. In general, after optical excitation the new angle of the easy axes $\Phi(t)$ is determined by $K_{c1}[T_0+\Delta T(t),\ p_0+\Delta p(t)]$ and $K_u[T_0+\Delta T(t),\ p_0+\Delta p(t)]$, where T_0 and p_0 are the initial (ambient) temperature and hole concentration. Thus the easy axis may assume a new direction immediately following photoexcitation if $\Delta T(t)$ or $\Delta p(t)$ is sufficiently large. This transient change in the magnetic easy axis, caused by the change in the minimum of the magnetic-free energy resulting from photoexcitation-induced Mn spin distribution, then triggers a precession of the ensemble of ferromagnetically coupled Mn spins (i.e., the magnetization of the system) around an effective magnetic field, and leads to an oscillatory behavior in the TRKR signal. Oscillations with relative long periods (~100 ps) that we ascribe to this process were observed previously by several groups.[11,12,15,16] However, whether $\Delta T(t)$ or $\Delta p(t)$ plays the dominant role in triggering the oscillation has remained an important unresolved issue.

B. TR-MOKE measurements at E_{ph} less than the GaAs bandgap E_g

Previously, all observations reported on the precession of magnetization in GaMnAs layers were obtained via the one-color pump-probe scheme using photon energies E_{ph} larger than the GaAs bandgap E_g. In the present study we have, in addition, covered the spectral range below E_g. Typical TRKR profiles below E_g are shown in Fig. 4 for sample B at 10 K for different polarizations of the excitation light. Similar re-

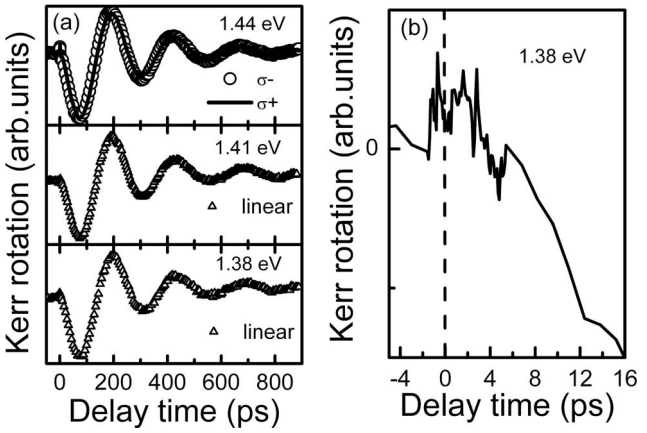

FIG. 4. (a) Temporal Kerr rotation profiles measured at 10 K at photon energies below band gap of GaAs for sample B; (b) temporal Kerr rotation profile at photon energy $E_{\mathrm{ph}}=1.38$ eV from (a) in the short-time domain. The dotted line is zero time delay where the pump and probe cross-correlation profile peaks. All results were obtained using a constant pump fluence I_0.

sults were observed in our experiments using other as-grown and annealed ferromagnetic GaMnAs samples. The data can be satisfactorily fitted by the equation,

$$\Delta\theta_K = A\,\exp(-t/\tau_d)\sin(\omega t+\phi). \tag{1}$$

These measurements clearly demonstrate that for a given E_{ph} below E_{g} with the same external conditions, only the purely oscillatory behavior is observed; and that all the carrier spin-related dynamics is greatly reduced or unnoticeable. This is consistent with the fact that for $E_{\mathrm{ph}}<E_{\mathrm{g}}$ no electrons are excited to the conduction band, and hence no Kerr rotation signal from the net coherent electron spins is obtained, in contrast to the situation for experiments at $E_{\mathrm{ph}}>E_{\mathrm{g}}$ described above. This observation confirms our interpretation that the polarization-dependent signal in Fig. 2 is due to conduction-band photoexcited electrons.

It should be noted here that in the GaMnAs samples grown by LT-MBE no distinct optical-absorption band gap has been clearly identified due to the presence of Mn dopants and point defects. Consequently, below-gap light absorption may be attributed to (a) the presence of defect states within the band gap (such as $\mathrm{As_{Ga}}$ antisites and $\mathrm{Mn_I}$ interstitials), (b) the breakdown of momentum conservation due to disorder, and (c) free-carrier absorption.[6,28] In these cases, both the local temperature and the local hole concentration may be enhanced by the incident laser pulses. As discussed above, both the increase in temperature and the increase in hole concentration can lead to the observed magnetization precession. In summary, the TRKR signal observed for below-gap photon absorption can be attributed entirely to ferromagnetically coupled Mn spins with no contribution from electron spins in the conduction band, for all polarizations of the pump light. We also note that the amplitude A of oscillations has no strong dependence on the probe polarization direction, indicating that the polar Kerr rotation (out-of-plane component of the magnetization) dominates the detected TRKR signal, and the contribution due to any possible mag-

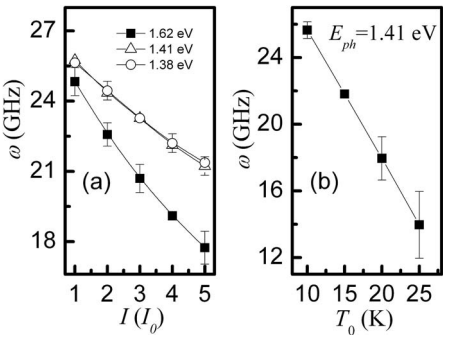

FIG. 5. Precession frequency ω in sample B as a function of (a) pump intensity at $T_0=10$ K; and (b) ambient temperature at $I=I_0$, respectively. Photon energy dependence of the precession frequency is also shown in (a). Note the difference between the precession frequencies for excitations above and below the band-gap energy.

netic linear dichroism can be neglected.[29] This excitation regime is therefore useful for the study of the precession of coherent Mn spins, exclusively.

In order to study differences in the effects observed with E_{ph} below or above the GaAs band gap, we carried out pump intensity and temperature-dependent measurements of the oscillatory behavior of TRKR for both cases on sample B. Figures 5 and 6 show the fitted oscillation frequency ω and amplitude A for sample B as a function of pump fluence (I) and ambient temperature (T_0), respectively. Our measurements show that the precession frequency ω decreases when either the pump intensity or the ambient temperature is increased. This indicates that the transient temperature rise induced by photoexcitation plays an important role in causing the oscillatory behavior. In Fig. 5(a), we also notice that the precession frequency for $E_{\mathrm{ph}}>E_{\mathrm{g}}$ is smaller than that for

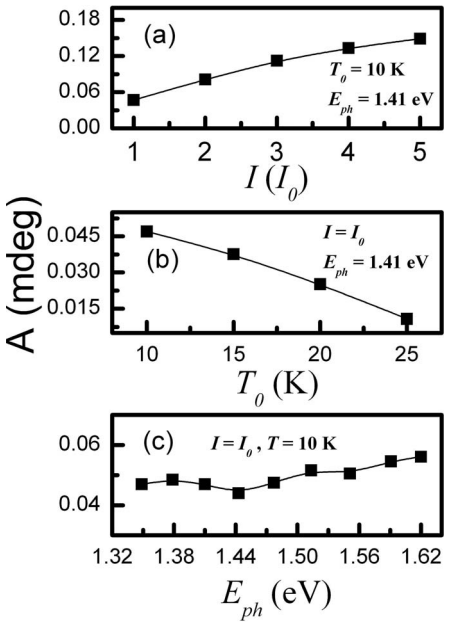

FIG. 6. Amplitude A in sample B as a function of (a) pump intensity at $T_0=10$ K and $E_{\mathrm{ph}}=1.41$ eV, (b) ambient temperature at $I=I_0$ and $E_{\mathrm{ph}}=1.41$ eV, and (c) photon energy at $T_0=10$ K and $I=I_0$, respectively.

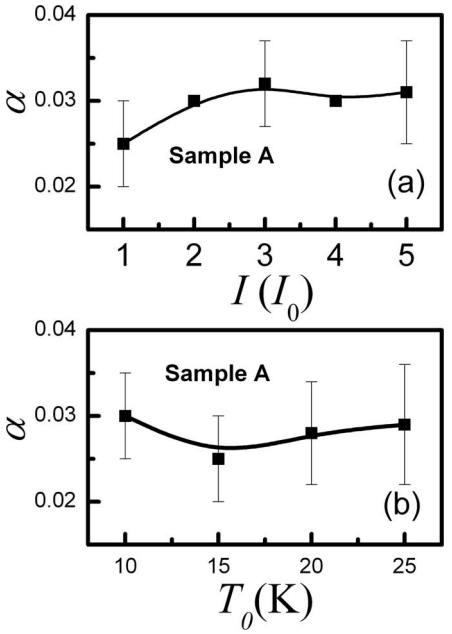

FIG. 7. Gilbert damping coefficient for sample A (annealed) as a function of (a) pump intensity I at $T_0=10$ K, and (b) ambient temperature T_0 at $I=I_0$. Here, $E_{\mathrm{ph}}=1.41$ eV.

$E_{\mathrm{ph}}<E_{\mathrm{g}}$ at the corresponding pump fluences. In addition, with increasing I, ω decreases at a greater rate for $E_{\mathrm{ph}}>E_{\mathrm{g}}$ than for $E_{\mathrm{ph}}<E_{\mathrm{g}}$. We also notice that for $E_{\mathrm{ph}}<E_{\mathrm{g}}$ the measured frequency at 10 K with excitation intensity $5I_0$ roughly equals the frequency at 15 K with pump fluence I_0. Thus, an estimate of the average light-induced temperature increase can be made to be $\Delta T\sim 1$ K for $T_0=10$ K and $I=I_0$. This causes a $\sim 2\%$ change in the anisotropy constants,[20] which is a small perturbation to the system. This small perturbation leads to a small but finite fluctuation in the magnetization at low pump fluences, and thus provides a basis for the theoretical analysis treated below.

IV. THEORETICAL MODEL

In the mean-field approximation the phenomenological Landau-Lifshitz-Gilbert (LLG) equation can be employed to describe the collective magnetization dynamics observe in our experiments. The LLG equation has the form

$$\frac{\partial \vec{M}}{\partial t} = -\gamma \vec{M} \times \vec{H}_{\mathrm{eff}} + \frac{\alpha}{M} \vec{M} \times \frac{\partial \vec{M}}{\partial t}, \tag{2}$$

where $\vec{M}$ is the local magnetization due to Mn ions, γ is the gyromagnetic ratio, $\vec{H}_{\mathrm{eff}}=-\partial E/\partial \vec{M}$ is the effective field given by the gradient of the magnetic energy E, and α is the Gilbert damping coefficient. The effective field $\vec{H}_{\mathrm{eff}}$ includes the external static magnetic field, as well as magnetic anisotropy and exchange fields.[6] The first term on the right-hand side (rhs) of Eq. (2) describes the precession of the magnetization, and the second term represents the relaxation of the collective magnetization motion. Figures 7–9 shows the numerically fitted Gilbert damping coefficient in samples A, B,

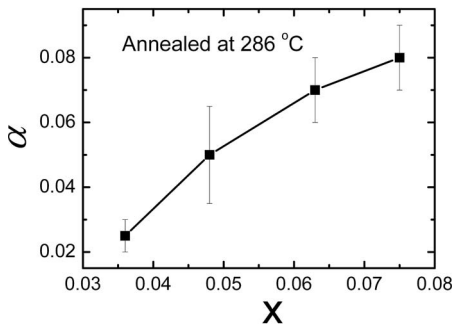

FIG. 8. Gilbert damping coefficient as a function of Mn concentration x for four $Ga_{1-x}Mn_xAs$ samples prepared under the same annealing conditions at $E_{\mathrm{ph}}=1.41$ eV, $T_0=10$ K, and $I=I_0$.

and several other annealed samples. It is shown below that α in the annealed sample is much smaller (about ten times) than that in the as-grown sample. A similar result was observed in FMR experiments.[30]

Since in this case there is no external applied magnetic field, within the mean-field treatment of the p-d magnetic exchange interaction, the average Mn spin $\langle \vec{S}_{\mathrm{Mn}} \rangle$ precesses around an effective magnetic field $\vec{H}_{\mathrm{eff}}$, which is mainly attributed to the anisotropy field $\vec{H}$ and the hole-spin mean field $\beta \langle \vec{s}_h \rangle$. The dynamics of the average hole spin $\langle \vec{s}_h \rangle$ is determined by its precession around the mean field $\beta N_{\mathrm{Mn}} \langle \vec{S}_{\mathrm{Mn}} \rangle$ due to the Mn spins, and by its rapid relaxation due to the strong spin-orbit interaction in the valence band, with a rate Γ of the order of tens of femtoseconds.[31,32] Here, β is the exchange constant and N_{Mn} is the number of substitutional Mn_{Ga} ions per unit volume. Due to the fact that hole-spin precession and relaxation are more rapid than any changes in the ferromagnetically coupled Mn spins, in the adiabatic limit the interplay between the exchange interaction in Eq. (2) and the carrier spin dephasing makes an contribution to magnetization damping.[19,33] This damping mechanism, arising from the p-d exchange interaction with the holes, is believed to be essential to the understanding of the intrinsic relaxation of ferromagnetic (III,Mn)V

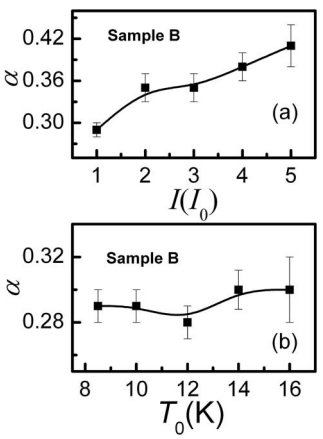

FIG. 9. Gilbert damping coefficient for sample B (as-grown) as a function of (a) pump intensity at $T_0=10$ K, and (b) ambient temperature at $I=I_0$. Here, $E_{\mathrm{ph}}=1.41$ eV.

semiconductors.[30] An effective LLG equation in the adiabatic limit can be written in the form[19,33]

$$\frac{\partial \vec{M}}{\partial t} = -\gamma_r \vec{M} \times \vec{H} + \frac{\alpha_r}{M} \vec{M} \times \frac{\partial \vec{M}}{\partial t}, \quad (3)$$

where γ_r and α_r include the kinetic-exchange contribution and other damping contributions.

The magnetic energy E can be expressed as follows:[20,25]

$$E(\vec{M}) = \frac{K_{c1}}{2}(\hat{M}_x^2 - \hat{M}_y^2)^2 + K_u(\hat{M}_x - \hat{M}_y)^2 + K_{uz}\hat{M}_z^2, \quad (4)$$

where $\hat{M} = \vec{M}/M$, and K_{uz} is the uniaxial anisotropy constant perpendicular to the film. We will use Eqs. (3) and (4) to obtain a qualitative picture of the dynamics of light-induced precession of magnetization occurring in the present experiments. Due to the initial in-plane magnetization in a compressively strained $Ga_{1-x}Mn_xAs/GaAs$ system,[6] we consider (assuming the x-y plane and the z axis to be parallel and perpendicular to the sample plane, respectively) a small perturbation of $M_x \approx M$ ($M_{y,z} \ll M$). Then, Eq. (3) is expanded into three components,

$$\frac{\partial M_x}{\partial t} = 0, \quad (5)$$

$$\frac{\partial M_y}{\partial t} = -2\gamma_r K_{uz} M_z - \alpha_r \frac{\partial M_z}{\partial t}, \quad (6)$$

$$\frac{\partial M_z}{\partial t} = -2\gamma_r K_u - 2\gamma_r K_{c1} M_y + \alpha_r \frac{\partial M_y}{\partial t}, \quad (7)$$

where we neglect second-order terms. Considering $K_{c1} < 0$ and $K_{uz} > 0$ (Ref. 6, 20, 25, and 26) and depending on initial conditions, the above equations have a solution of the form

$$M_y = A\cos(\omega t + \varphi)e^{-t/\tau}, \quad M_z = A\eta \sin(\omega t)e^{-t/\tau}, \quad (8)$$

where

$$\omega = \gamma_r \frac{\sqrt{-4K_{c1}K_{uz} - \alpha_r^2(K_{uz} + K_{c1})^2}}{1 + \alpha_r^2}, \quad \tau = \frac{2(1 + \alpha_r^2)}{\alpha_r \gamma_r (K_{uz} - K_{c1})}. \quad (9)$$

According to Eq. (8), when measuring the y or z component of magnetization in time domain after a small perturbation of the initial magnetic equilibrium state, one expects to obtain a sine- or cosinelike signal with a precession frequency ω and an exponential decay characterized by a decay time τ. This is consistent with Eq. (1). It can be seen that the precession frequency ω is closely related to the anisotropy constants (e.g., K_{c1} and K_{uz}), which also directly connect the Gilbert damping coefficient with the exponential decay time. Since $\alpha_r^2 \ll 1$ (see also Figs. 6–8), terms associated with α_r^2 can be neglected in the expression for ω in Eq. (9).

V. DISCUSSION

A. Precessional frequency ω and amplitude A

Equations (8) and (9) can readily account for the results presented in Figs. 4 and 5. Below T_C, it is known that $|K_{c1}|$ and K_{uz} increase with decreasing temperature.[20,25–27] Thus, according to Eq. (9), ω is expected to decrease as $|K_{c1}|$ and K_{uz} are reduced. This conclusion is seen to agree with the results in Fig. 5, which shows that ω becomes smaller either as we raise the ambient T_0 or as we increase $\Delta T(t)$ by increasing the pump fluence I. One should note here that, in principle, increasing the hole concentration could also decrease $|K_{c1}|$,[27] which could then lead to a decrease in ω. However, in our experiments $\Delta p/p_0$ is about 3 or 4 orders of magnitude smaller than $\Delta T/T_0$. We can therefore conclude that the transient temperature change, not changes in the hole concentration, plays the dominant role in accounting for the observed oscillatory behavior in the TRKR signal. The fact that the observed precession behavior seen in Fig. 4(b) begins after a delay of about 4 ps strongly supports this conclusion.

When the photon energy E_{ph} is somewhat above the GaAs band gap E_g, in thin GaMnAs samples (on the order of 100 nm or less), the incident pump light is absorbed not only by the top GaMnAs layer but also by the LT-GaAs and GaAs buffer layers in addition to the GaAs substrate. This follows since the penetration depth is of the order of a micrometer, as deduced from the absorption coefficient. In this case, the local transient temperature change has a contribution from the photon energy in excess of the band-gap energy for all layers. This above band-gap contribution is expected to be larger than the below band-gap contribution characterized above. For example, at $E_{ph} = 1.62$ eV, ΔT is estimated to be ~ 3 K with $T_0 = 10$ K and $I = I_0$, which is three times larger than the case where $E_{ph} = 1.38$ eV. This effect may be more significant at large pump fluences, resulting in the frequency of oscillation becoming smaller. This is clearly demonstrated in the measurements shown in Fig. 5(a). Our data thus indicate that for relatively strong photoexcitation at $E_{ph} > E_g$ the observed dynamics in the top ferromagnetic GaMnAs layer is likely to have an additional contribution from the underlying layers. One way to eliminate this effect is to work with low E_{ph} (much smaller than E_g), as illustrated above; or to use sufficiently high pump photon energy so that the penetration depth is of the order of the GaMnAs thickness.

As can be seen in Fig. 6, the amplitude of the oscillations increases rapidly as the pump intensity increases or as the ambient temperature decreases. This result is also in accord with the above-proposed model due to the fact that the dominant relative change $\Delta T/T_0$ increases as T_0 decreases or as I increases, and leads to an increase in the magnitude of Φ or to a photoinduced tilt in the easy axis. Such increased Φ or tilt in the easy axis results in the increasing of the initial out-of-plane component of the subsequent precessional magnetization, reflected by the amplitude of the oscillations, as shown in Fig. 6. As seen in Fig. 6(c), the magnitude of A is only weakly sensitive to changes in photon energy. The amplitude A does also show a tendency to increase slowly as E_{ph} increases when $E_{ph} > E_g$. This may be understood as re-

sulting from local increases in temperature at high E_{ph} due to optical absorption, as was discussed in the preceding paragraph.

B. Magnetization relaxation

We now turn to our measurements of oscillation damping, which is intimately related to the lifetime of the excited collective spins. When ferromagnetism is hole mediated, as in the GaMnAs system, spin scattering between the local Mn spins and the hole spins can lead to the relaxation of the collective (hole-and-Mn) magnetic moment.[19,30,33,34] This gives an intrinsic contribution to the Gilbert damping coefficient. This contribution can be deduced from the adiabatic-limit approximation to be[19]

$$\alpha_{pd} = \frac{\gamma s_{\parallel}}{M} \frac{\Gamma_{\perp} h_{\mathrm{eff}}}{(h_{\mathrm{eff}} + h_{\parallel})^2 + \Gamma_{\perp}^2}, \tag{10}$$

where $\Gamma_{\perp}(=2\Gamma_{\parallel})$ is the hole-spin transverse relaxation rate, $h_{\mathrm{eff}}=\beta N_{\mathrm{Mn}} S_{\mathrm{Mn}}$, $s_{\parallel}=\vec{s}_h \cdot \vec{S}_{\mathrm{Mn}}/S_{\mathrm{Mn}}$, and $h_{\parallel}=\gamma \vec{H} \cdot \vec{S}_{\mathrm{Mn}}/S_{\mathrm{Mn}} \approx 0$. In the annealed samples the Gilbert damping coefficient deduced from TRKR experiments is around 0.03, which is close to the value estimated from Eq. (10).[33] Thus, in this case, we anticipate that the damping mechanism due to the kinetic-exchange interaction dominates the precession damping.[30] In the annealed sample A, we measured α as a function of the pump intensity I and the ambient temperature T_0, respectively (see Fig. 7). As already mentioned, for the pump intensity range used in current experiments the transient increase in the local hole density is very small. Under these circumstances one would not expect significant changes in the parameters of Eq. (10), and hence in the damping coefficient α_{pd}, associated with changes in hole concentration. This is consistent with the results shown in Fig. 7(a). On the other hand, when the ambient temperature is increasing, the ratio $s_{\parallel}/M$ may increase nonlinearly with increasing temperature[35] but h_{eff} will decrease. This may explain the observed result in Fig. 7(b) that α is almost constant as a function of T_0. Figure 8 shows α as a function of Mn concentration x. All samples with differing Mn concentration x in Fig. 8 were prepared under the same growth and annealing conditions as sample (A), and have the same film thickness as that sample. Their Curie temperatures are: $T_C \sim 80$ K for $x \sim 0.036$; $T_C \sim 86$ K for $x \sim 0.048$; $T_C \sim 105$ K for $x \sim 0.065$; and $T_C \sim 115$ K for $x=0.075$. It is clearly seen that both α and the Curie temperature increase with increasing x. This result, when the Mn concentration $x<8\%$, may be due to the fact that h_{eff} increases with increasing hole concentration, which reflects the coupling between the exchange interaction and hole density.[30]

In contrast, in the as-grown samples the Gilbert damping coefficient is seen to reach values of around 0.3, which is much higher than what the intrinsic kinetic-exchange mechanism predicts. This indicates that other damping mechanisms must take over. Classically, the most probable mechanism is the spin dephasing process characterized by T_2, in which the coherent spins, initially precessing in phase, lose their phase due to spatial and temporal fluctuations in the precession frequencies.[36] These fluctuations are mainly attributed to local small-scale field inhomogeneities, which are created by magnetic defects, domain walls, etc. Quantum mechanically, such dephasing can be primarily attributed to two-magnon scattering,[37] where an excited magnon mode (created by photoexcitation) scatters on other magnons having the same frequency (degenerate magnons) without requiring conservation of the magnon momentum. In as-grown $Ga_{1-x}Mn_xAs$ fabricated by low-temperature MBE, large numbers of defects, such as As_{Ga} antisites and Mn_I interstitials, are invariably present. In particular, interstitial Mn_I ions tend to be antiferromagnetically coupled to substitutional Mn_{Ga}, which can greatly affect the local magnetic properties.[6] Such Mn_I-induced magnetic defects can then alter the local magnetic landscape, leading to extrinsic dephasing effects. Removing the Mn_I—as is done in postgrowth annealing—should then increase the magnetization relaxation time. This effect has been clearly demonstrated in our experiments.

In particular, our results indicate that this dominant extrinsic mechanism in as-grown samples is also relatively independent of the ambient temperature (within the temperature range of our experiments) but is significantly enhanced as we increase the pump intensity (see Fig. 9). If we assume the local precession frequency $\omega(\vec{r},t)$ and the effective field $h[T(\vec{r},t)]$ to be temperature dependent, then the dephasing effect can be parameterized in terms of the quantity $\delta\omega$ as follows:

$$\delta\omega = \gamma \frac{\partial h}{\partial T} \frac{\partial T}{\partial \vec{r}} \delta\vec{r} + \gamma \frac{\partial h}{\partial T} \frac{\partial T}{\partial t} \delta t. \tag{11}$$

If the ambient temperature T_0 is kept constant, increasing the pump fluence can significantly increase $\partial T/\partial \vec{r}$ and $\partial T/\partial t$, and hence also increase $\delta\omega$, which results in the observed enhancement of dephasing. In comparison, $\partial h/\partial T_0$ should change little in the relevant temperature range. To our knowledge, up to now there have been no theoretical studies of damping of magnetization dynamics related to the local effects of interstitial Mn_I. However, our results obtained on as-grown and annealed GaMnAs clearly point to a connection between extrinsic dephasing effects and the local Mn_I distribution; and it is therefore hoped that these results should stimulate the interest of theorists in addressing this problem.

VI. CONCLUSIONS

In this paper we report a study of photoinduced coherent spin dynamics in ferromagnetic GaMnAs using time-resolved magneto-optical spectroscopy. Our observations identify distinctive contributions to the observed temporal magneto-optical signals which arise either from coherent electron spins excited in the conduction band by polarized optical pumping, or from ferromagnetically coupled Mn spins. For the case of electron spin, we observe that they are decoupled from the local Mn moments, and that they persist over the entire temperature range of our experiments, from 10 K to room temperature. At low temperatures (below the Curie temperature of GaMnAs) we observed oscillations that arise from precession of the ferromagnetically coupled Mn

spins. We have derived an effective Landau-Lifshitz-Gilbert-type equation based on the mean-field theory to describe the observed magnetization precession. The precession can be primarily attributed to magnetic anisotropy changes in the GaMnAs system due to transient temperature increases produced by the optical pump. Our studies of the Gilbert damping coefficient, as function of the pump intensity, temperature, and the Mn concentration in annealed and as-grown samples, allow us to identify and characterize several important damping mechanisms arising from the intrinsic *p-d* exchange interactions and to extrinsic dephasing effects.

ACKNOWLEDGMENTS

This work was supported by DOE through Grant No. DE-FGO2-99ER45781 (Vanderbilt), NSF under Grant No. DMR06-03752 (Notre Dame), and by EU STREP program HYSWITCH (Crete).

[1] B. Koopmans, M. van Kampen, and W. J. M. de Jonge, J. Phys.: Condens. Matter **15**, S723 (2003).
[2] K. H. Bennemann, J. Phys.: Condens. Matter **16**, R995 (2004).
[3] J. Wang, C. Sun, Y. Hashimoto, J. Kono, G. A. Khodaparast, L. Cywinski, L. J. Sham, G. D. Sanders, C. J. Stanton, and H. Munekata, J. Phys.: Condens. Matter **18**, R501 (2006).
[4] A. V. Kimel, A. Kirilyuk, F. Hansteen, R. V. Pisarev, and Th. Rasing, J. Phys.: Condens. Matter **19**, 043201 (2007).
[5] H. Ohno, Science **281**, 951 (1998).
[6] J. Jungwirth, J. Sinova, J. Masek, J. Kucera, and A. H. MacDonald, Rev. Mod. Phys. **78**, 809 (2006).
[7] E. Kojima, R. Shimano, Y. Hashimoto, S. Katsumoto, Y. Iye, and M. Kuwata-Gonokami, Phys. Rev. B **68**, 193203 (2003).
[8] E. Kojima, J. B. Héroux, R. Shimano, Y. Hashimoto, S. Katsumoto, Y. Iye, and M. Kuwata-Gonokami, Phys. Rev. B **76**, 195323 (2007).
[9] A. V. Kimel, G. V. Astakhov, G. M. Schott, A. Kirilyuk, D. R. Yakovlev, G. Karczewski, W. Ossau, G. Schmidt, L. W. Molenkamp, and T. Rasing, Phys. Rev. Lett. **92**, 237203 (2004).
[10] Y. Mitsumori, A. Oiwa, T. Słupinski, H. Maruki, Y. Kashimura, F. Minami, and H. Munekata, Phys. Rev. B **69**, 033203 (2004).
[11] A. Oiwa, H. Takechi, and H. Munekata, J. Supercond. **18**, 9 (2005).
[12] Y. Hashimoto, S. Kobayashi, and H. Munekata, Phys. Rev. Lett. **100**, 067202 (2008).
[13] J. Wang, I. Cotoros, K. M. Dani, X. Liu, J. K. Furdyna, and D. S. Chemla, Phys. Rev. Lett. **98**, 217401 (2007).
[14] J. Wang, Ł. Cywiński, C. Sun, J. Kono, H. Munekata, and L. J. Sham, Phys. Rev. B **77**, 235308 (2008).
[15] J. Qi, Y. Xu, N. H. Tolk, X. Liu, J. K. Furdyna, and I. E. Perakis, Appl. Phys. Lett. **91**, 112506 (2007).
[16] E. Rozkotova, P. Němec, P. Horodyská, D. Sprinzl, F. Trojánek, P. Malý, V. Novák, K. Olejník, M. Cukr, and T. Jungwirth, Appl. Phys. Lett. **92**, 122507 (2008).
[17] Ł. Cywiński and L. J. Sham, Phys. Rev. B **76**, 045205 (2007).
[18] J. Chovan, E. G. Kavousanaki, and I. E. Perakis, Phys. Rev. Lett. **96**, 057402 (2006).
[19] J. Chovan and I. E. Perakis, Phys. Rev. B **77**, 085321 (2008).
[20] U. Welp, V. K. Vlasko-Vlasov, X. Liu, J. K. Furdyna, and T. Wojtowicz, Phys. Rev. Lett. **90**, 167206 (2003); J. K. Furdyna, X. Liu, W. L. Lim, Y. Sasaki, T. Wojtowicz, I. Kuryliszyn, S. Lee, K. M. Yu, and W. Walukiewicz, J. Korean Phys. Soc. **42**, S579 (2003).
[21] *Optical Orientation*, edited by F. Meier and B. P. Zakharchenya (North-Holland, New York, 1984).
[22] G. E. Pikus, V. A. Marushchack, and A. N. Titkov, Sov. Phys. Semicond. **22**, 115 (1988).
[23] D. J. Hilton and C. L. Tang, Phys. Rev. Lett. **89**, 146601 (2002).
[24] A. V. Kimel, V. V. Pavlov, R. V. Pisarev, V. N. Gridnev, F. Bentivegna, and Th. Rasing, Phys. Rev. B **62**, R10610 (2000).
[25] X. Liu, Y. Sasaki, and J. K. Furdyna, Phys. Rev. B **67**, 205204 (2003).
[26] X. Liu, W. L. Lim, M. Dobrowolska, J. K. Furdyna, and T. Wojtowicz, Phys. Rev. B **71**, 035307 (2005).
[27] K. Hamaya, T. Watanabe, T. Taniyama, A. Oiwa, Y. Kitamoto, and Y. Yamazaki, Phys. Rev. B **74**, 045201 (2006).
[28] E. J. Singley, K. S. Burch, R. Kawakami, J. Stephens, D. D. Awschalom, and D. N. Basov, Phys. Rev. B **68**, 165204 (2003).
[29] A. V. Kimel, G. V. Astakhov, A. Kirilyuk, G. M. Schott, G. Karczewski, W. Ossau, G. Schmidt, L. W. Molenkamp, and Th. Rasing, Phys. Rev. Lett. **94**, 227203 (2005).
[30] J. Sinova, T. Jungwirth, X. Liu, Y. Sasaki, J. K. Furdyna, W. A. Atkinson, and A. H. MacDonald, Phys. Rev. B **69**, 085209 (2004).
[31] T. Dietl, H. Ohno, and F. Matsukura, Phys. Rev. B **63**, 195205 (2001).
[32] M. Abolfath, T. Jungwirth, J. Brum, and A. H. MacDonald, Phys. Rev. B **63**, 054418 (2001).
[33] Y. Tserkovnyak, G. A. Fiete, and B. I. Halperin, Appl. Phys. Lett. **84**, 5234 (2004).
[34] M. D. Kapetanakis and I. E. Perakis, Phys. Rev. Lett. **101**, 097201 (2008).
[35] S. Das Sarma, E. H. Hwang, and A. Kaminski, Phys. Rev. B **67**, 155201 (2003).
[36] F. Bloch, Phys. Rev. **70**, 460 (1946).
[37] M. Sparks, *Ferromagnetic Relaxation Theory* (McGraw-Hill, New York, 1966), pp. 18–34.